

# Structure and Thermal Behaviour of Nylon 6 Nanocomposites

Xiong-Yan Zhao,<sup>1</sup> Ming-Zhu Wang<sup>2</sup>

<sup>1</sup>College of Material Science and Engineering, Hebei University of Science and Technology, Shijiazhuang 050054, People's Republic of China

<sup>2</sup>Hebei Province Analysis and Testing Research Centre, Hebei University of Science and Technology, Shijiazhuang 050018, People's Republic of China

Received 3 March 2005; accepted 24 June 2005

DOI 10.1002/app.22530

Published online in Wiley InterScience (www.interscience.wiley.com).

**ABSTRACT:** In this article, nylon 6/clay nanocomposites with 5 wt % clay (NCN5) were prepared by a twin screw extruder. The effects of annealing including solid-state annealing (170 and 190°C) and melt-state annealing (240°C) on the polymorphic behavior and thermal property of NCN5 and nylon 6 have been comparatively studied as a function of annealing time using modified differential scanning calorimetry (MDSC) and wide-angle X-ray diffraction. It was demonstrated that NCN5 and nylon 6 exhibit a similar polymorphic behavior when they were annealed at 190°C for different time durations. As the annealing temperature was elevated to 240°C, significant differences in thermal behavior and polymorphism between NCN5 and nylon 6 could be

found. For example, the  $\alpha$  crystal became the absolutely dominating crystalline phase for NCN5 sample independent on the annealing durations, whereas the formation of  $\gamma$  crystal is greatly enhanced in neat nylon 6 with increasing annealing time. Moreover, a small endothermic peak is observed around 180°C in both nylon 6 and NCN5 samples annealed at 170 and 190°C, which might be related to the melting of microcrystals formed in the amorphous regions during annealing. © 2006 Wiley Periodicals, Inc. *J Appl Polym Sci* 100: 3116–3122, 2006

**Key words:** nylon 6; nylon 6/clay nanocomposites; annealing; crystal structure

## INTRODUCTION

The study of organic–inorganic nanocomposites is an emerging field of investigation. Polymer clay nanocomposites represent a new class of materials where nanoscale clay particles are uniformly dispersed in a polymer matrix. The property improvements for organic–inorganic nanocomposites can generally be classified into the following aspects, including (1) dramatically improved mechanical properties,<sup>1,2</sup> (2) heat resistance,<sup>3–5</sup> (3) dimensional stability,<sup>6</sup> (4) superior barrier to gas and water,<sup>6,7</sup> and (5) flame retardation.<sup>8,9</sup> Thus today, one of the exciting and promising developments in material science is the design and synthesis of organic–inorganic nanocomposites that possess enhanced and novel properties, which are impossible in the individual organic and inorganic materials.<sup>10–13</sup> With the development of nylon 6/clay nanocomposites by Tyoto Research Centre,<sup>1,2</sup> there have been increasing attentions to this system in the past decade.<sup>14–20</sup> As we know, one of the most remarkable features of nylon 6 is that these semicrystalline polymers exhibit polymorphism depending on the thermal

history, processing conditions, mechanical stress, and crystallization condition. Since the importance of polymorphic form on elevated temperature properties, such as heat distortion temperature, softening, dimensional stability, and warp, the polymorphism and polymorphic transformations of nylon 6 nanocomposites have drawn much considerable research interests. Studies on the crystal structure of nylon 6 in nanocomposites were first carried by Kojima et al.,<sup>21</sup> who reported that both  $\alpha$  and  $\gamma$  crystals were present in nanocomposites. However, after annealing under elevated pressure, they found that the fraction of  $\gamma$ -phase decreased. The nonisothermal crystallization studies on polyamide/clay nanocomposites by Liu et al.<sup>22</sup> showed that the addition of silicate layers favored the formation of the  $\gamma$ -crystalline form. Mathias et al.<sup>15</sup> reported that when both crystal forms were present in nanocomposites, those annealed at 200°C under vacuum produced only  $\gamma$  crystals. Fornes and Paul<sup>23</sup> found that there were significant differences in crystal type within the core and skin regions of injection-molded nanocomposites. The skin region contains only the  $\gamma$ -crystalline form; the core region, on the other hand, contains both  $\alpha$ - and  $\gamma$ -forms of nylon 6. Wu et al.<sup>18</sup> showed from his DSC and XRD results that the polymorphic behavior in nylon 6/clay nanocomposites depend on the content of clay and the cooling rate from melt. Thermal treatment of nylon 6 and

Correspondence to: X.-Y. Zhao (zhaoxy@hebust.edu.cn).

nylon 6/clay nanocomposites at various temperatures promotes mostly the  $\alpha$  form crystalline formation. Okamoto et al.<sup>24</sup> investigated the effect of crystallization temperature ( $T_c$ ) on crystal structure of nylon 6 and its nanocomposite. Their results show that at lower  $T_c$ , both  $\alpha$  and  $\gamma$  crystal structures are formed in nylon 6, with increasing  $T_c$ , the  $\gamma$ -form gradually disappeared. On the other hand, only the  $\gamma$  crystal is pronounced for the nylon 6 nanocomposites throughout the whole  $T_c$  range studied. Although intensive research efforts have been devoted to this system, to our knowledge, most research mainly focus on the effect of clay and the annealing temperature on crystallization behavior of nylon 6 matrix.<sup>5,14–20,25,26</sup> The effect of annealing on thermal behavior of nylon 6/clay nanocomposites is still an interesting subject needed to be further identified, since some microstructural changes may occur at such high annealing temperature, which would have a significant impact on properties of nylon 6/clay nanocomposites.

In this work, a comparative study of the thermal property of pure nylon 6 and nylon 6/clay nanocomposites (NCN5) was carried out. In particular, we will focus our attention on the investigation of the effects of annealing conditions on the time evolution of the polymorphic structure of nylon 6 matrix in nylon 6 nanocomposites and to understand whether and how the thermal history affects the thermal property of nanocomposites.

## EXPERIMENTAL

### Materials

Nylon 6 (SF 1018A) with a molecular weight of 18,000 was purchased from UBE Industries Ltd., and its degree of crystallinity measured by XRD is 37.5%. Clay used in this research is montmorillonite mineral modified by Nanomer® I.30TC. Before extrusion, both nylon 6 and montmorillonite mineral were dried under vacuum at 100°C for 48 h. The nylon 6 nanocomposite with 5 wt % clay (NCN5) was prepared by a Leistritz Mic 18/G1–30D twin screw extruder. Each sample was extruded twice. The obtained samples were cut into small pieces and then dried under vacuum at 80°C for 24 h. The dried samples were melted in metal molder under N<sub>2</sub> at 260°C for about 8 min to eliminate the thermal history of samples. Finally, the samples were naturally cooled down to room temperature.

### Characterization

Modified differential scanning calorimetry (MDSC) (2920 Modulated DSC, TA Instrument) was used to analyze the thermal transition behaviors of the samples. MDSC is a relatively new technique that subjects a sample to a linear heating ramp with a superim-

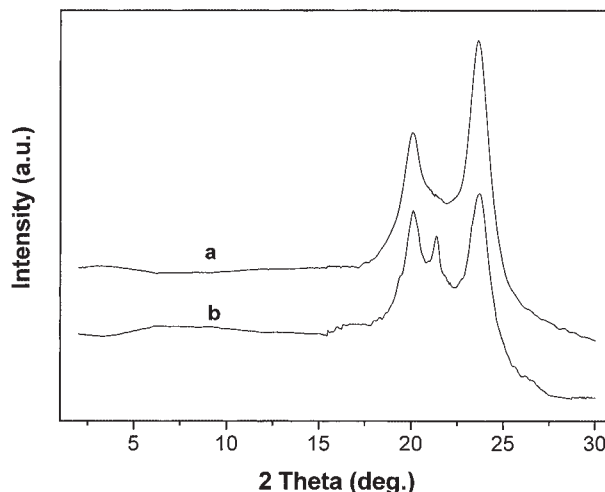
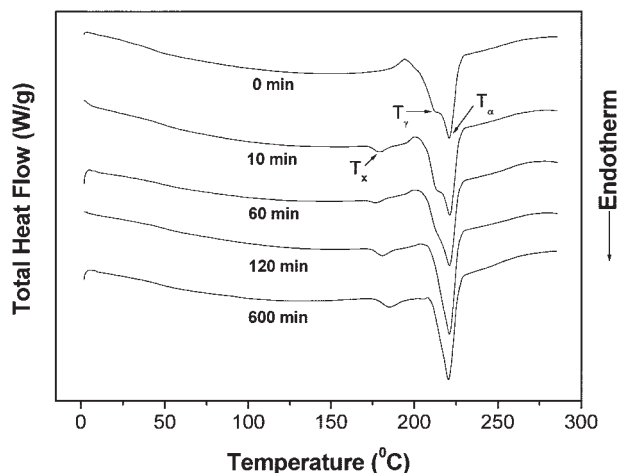


Figure 1 WAXD patterns of (a) neat nylon 6 and (b) NCN5.

posed low frequency temperature oscillation (modulation), resulting in a modulation in the heating profile. It could make the total heat flow to be separated into the heat capacity-related (reversible) and kinetic (nonreversible) components. Thus, the endothermic signals can be detected in both reversible and nonreversible scans, whereas the crystallization exotherms only contribute to the nonreversible signal. This makes MDSC a very powerful technique for the separation of exotherms (including crystallization and recrystallization) from reversible melting or other heat capacity-related events. All MDSC runs were made under a nitrogen atmosphere with heating and/or cooling rates of 5°C/min, and the thermal histories (namely, annealing temperature and the duration of annealing) of the specimens were varied. The MDSC was carefully calibrated for temperature and heat flow, following the standard procedures. The thermal transitions are reported as the maximum or minimum of the endothermic or exothermic peaks, respectively. To avoid any influence of previous thermal history, every sample was used only once. Wide-angle X-ray diffraction (WAXD) patterns were taken on a Rigaku RINT 2200 X-ray diffractometer, with Cu  $\alpha$  radiation, 40.0 kV, and 30.0 mA.

## RESULTS AND DISCUSSION

Figure 1 illustrates the X-ray diffraction patterns of neat nylon 6 and NCN5. It can be seen from Figure 1 that for neat nylon 6, two reflections have been observed at  $2\theta = 20.2^\circ$  and  $24.3^\circ$  corresponding to  $\alpha_1$  and  $\alpha_2$ , respectively,  $\alpha_1$  originates from the distance between hydrogen-bonded chains, whereas  $\alpha_2$  comes from the distance between hydrogen-bonded sheets. This indicates that the  $\alpha$ -phase is the dominant crystalline phase for neat nylon 6. For NCN5 samples,



**Figure 2** MDSC traces of neat nylon 6 annealed at 170°C for different time durations.

however, in addition to the two reflections as in neat nylon 6, another reflection is also detected at  $2\theta = 21.5^\circ$ , which is related to  $\gamma$  crystal planes of nylon 6. Thus, the addition of silicates into neat nylon 6 could favor the formation of  $\gamma$ -phase crystal. In addition, the fact that there is no peak existing at  $2\theta < 5^\circ$  indicates that an exfoliated structure has been formed in nanocomposite NCN5.

Annealing studies were carried out at different temperatures ( $T_a$ ) to have a deeper understanding of the differences between neat nylon 6 and NCN5 and the effect of thermal history on their phase behavior and structures. The samples were first heated to the annealing temperature at 40°C/min, then maintained at this temperature for a given duration, and then cooled to the room temperature at the same rate (40°C/min). Finally, the sample was heated from room temperature to the designated temperature at the rate of 5°/min. To better investigate the thermal and crystal morphological properties during annealing, three different annealing temperatures were chosen carefully in this study, i.e., 170 and 190°C (below  $T_{\gamma}$  solid-state annealing), and 240°C (above  $T_{\gamma}$  and  $T_{\alpha}$  melt-state annealing).

Figure 2 gives the traces of MDSC thermograms of neat nylon 6 specimens after annealing at 170°C for different times. It can be seen from Figure 2 that three different transitions appeared in nylon 6 MDSC thermograms. In addition to the presence of a sharp endothermic peak at 221°C assignable to the melting of  $\alpha$ -form crystals of nylon 6,<sup>14,16,27,28</sup> another two endotherms were also detected. There are a broad and less pronounced endothermic shoulder around 212°C and a broad but distinct endothermic peak centered around 180°C. The former is associated with the melting of  $\gamma$ -form crystals of nylon 6.<sup>29</sup> A remarkable feature in Figure 2 is the appearance of a small low-

temperature endothermic peak in all the materials annealed at 170 and 190°C.

It has been reported<sup>30–32</sup> that the most plausible reason for such behavior might be related to an enthalpy relaxation process of an interphase between the crystalline and amorphous phases, which can be induced by isothermal crystallization or annealing process. However, our results do not support this speculation, since this endothermic peak can also be detected in the reversing MDSC signal. So this endothermic behavior might be an indication of the melting of microcrystals formed in the amorphous regions during annealing. However, these peaks do not appear in the MDSC scans of the materials annealed at 240°C. This could be because the small endothermic peak is overshadowed by the melting of  $\gamma$ -crystal and  $\alpha$ -crystal. It is also possible that microcrystals do not form when annealing occurs near the melting point. To distinguish the three endothermic peaks appeared in nylon 6 and NCN5 during heating run, their temperatures were defined as  $T_{\gamma}$  for the melting peak of  $\gamma$ -form crystals,  $T_{\alpha}$  for the melting peak of  $\alpha$ -form crystals, and  $T_x$  for the low-temperature annealing peak, respectively. The corresponding heats of melting transition were named as  $\Delta H_{\gamma}$ ,  $\Delta H_{\alpha}$ , and  $\Delta H_x$ , respectively.

It is also worthwhile to note from Figure 2 that the  $\alpha$ -form crystal is the most predominant phase and melting peaks corresponding to  $\alpha$ -form crystals are greatly enhanced with increasing annealing time, whereas the melting peaks corresponding to  $\gamma$ -form crystals are observed only as a less pronounced shoulder and finally disappeared as the annealing times exceeded 60 min. This is not surprising, since, in solid state, polymer chains or segments are allowed to arrange themselves into a better organization when suitable conditions such as temperature and time are given to keep the system in a relatively lower energy. Furthermore, it can also be seen that the peak temperatures,  $T_{\alpha}$ , remained fairly constant independent of annealing time, but  $T_x$  for the low-temperature endothermic peak shifts to higher temperature with increasing annealing time. Meanwhile, its enthalpy of transition,  $\Delta H_x$ , increased steadily with increasing annealing time. The increase in both  $T_x$  and  $\Delta H_x$  appears to indicate that this annealing temperature could lead to an increase in crystalline perfection of microcrystals with increasing annealing time, probably due to the fact that the longer annealing duration could provide more time to relieve the microcrystal defects.

The MDSC thermograms of NCN5, annealed at 170°C for various durations, are illustrated in Figure 3. It is clear from Figure 3 that peak temperature  $T_{\alpha}$  of NCN5 specimens showed no change and the peak area also remain virtually constant after the specimen were annealed at 170°C for different periods of time. This suggests that annealing at 170°C has no signifi-

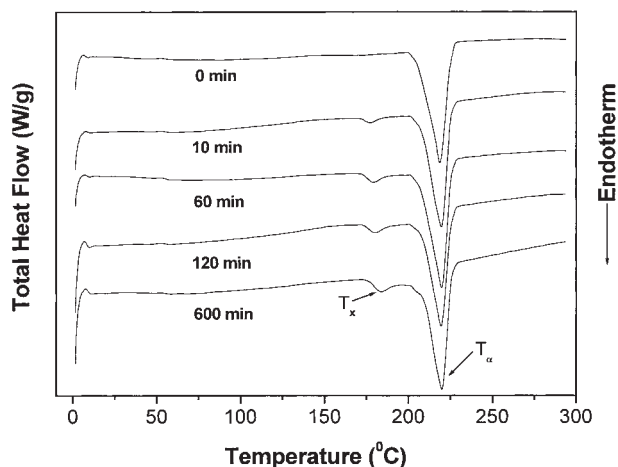


**Figure 3** MDSC traces of NCN5 annealed at 170°C for different time durations.

cant effects on the polymorphic structure of NCN5. Hence, thermodynamically stable  $\alpha$ -phase is expected as the predominant phase. Furthermore, the peak temperature of annealing peak,  $T_x$ , and its associated melt enthalpy,  $\Delta H_x$ , increased gradually with increasing annealing time, similar to that observed for neat nylon 6 annealed at the same temperature.

The different thermal events between NCN5 and nylon 6 are seen more clearly in Figures 4 and 5, which show the nonreversing MDSC signal of both samples. For NCN5, both exothermic and endothermic nonreversible events were detected simultaneously: a strong exotherm centered at 216°C, immediately followed by a sharp endothermic peak at 223°C, indicating that the  $\alpha$ -phase crystals undergo a process of crystal perfection during the heating scan and subsequently these higher melting species melt at 223°C. In addition, it can be seen from Figure 3 that annealing at 170°C has

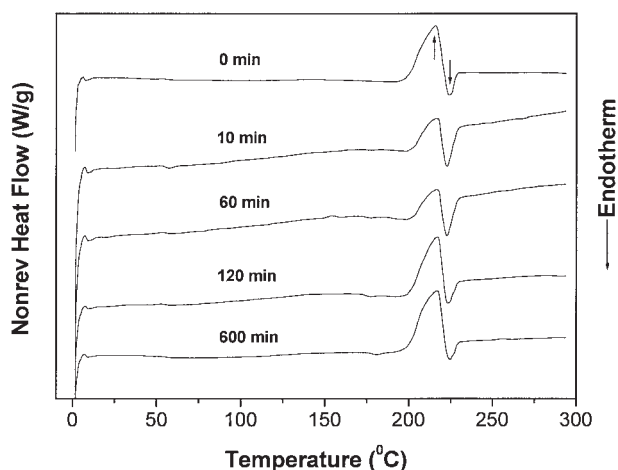


**Figure 4** Nonreversing MDSC data of NCN5 annealed at 170°C for different time durations.

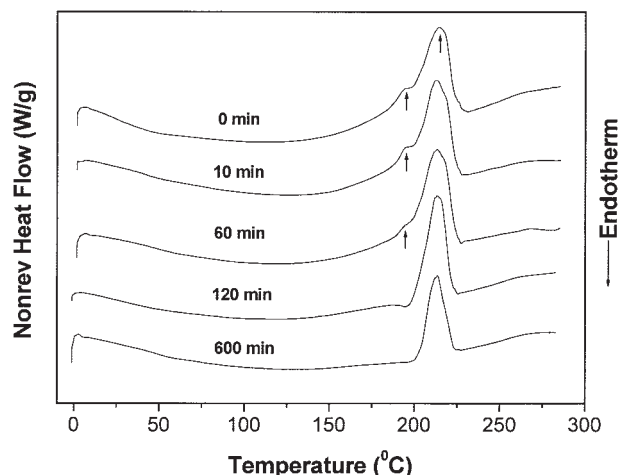


**Figure 5** Nonreversing MDSC data of neat nylon 6 annealed at 170°C for different time durations.

no appreciable effects on the crystal perfection process of nylon 6/clay nanocomposites. For neat nylon 6, however, two crystalline perfection processes seem to have appeared in the nonreversing exothermic signal (Fig. 5). There is a pronounced exotherm (216°C) overlapping with a small but distinct exotherm centered around 194°C. The former might be associated with the crystal perfection process of  $\alpha$ -crystal, while the latter is probably attributed to the crystal perfection process of  $\gamma$ -crystal. Moreover, it is also clear from Figure 5 that as the annealing durations exceeded 60 min, the small exothermic peaks corresponding to  $\gamma$ -crystal perfection process exist no more, which agrees well with Figure 2 results.

The MDSC traces of both NCN5 and neat nylon 6, annealed at 190°C for various times, are shown in Figures 6 and 7, respectively. The following observations are worth noting in Figure 6. (1) After being

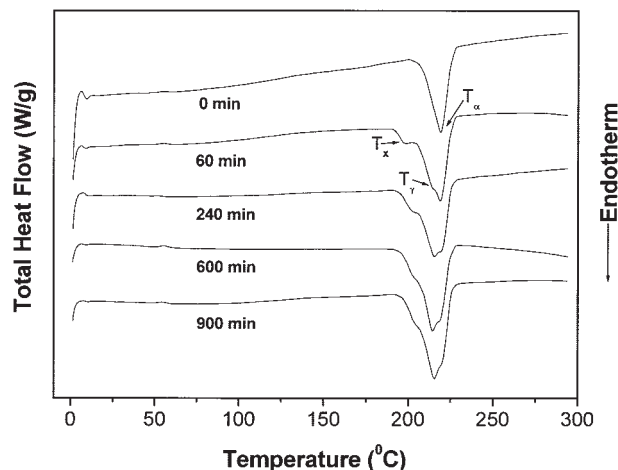


**Figure 6** MDSC traces of NCN5 annealed at 190°C for different time durations.

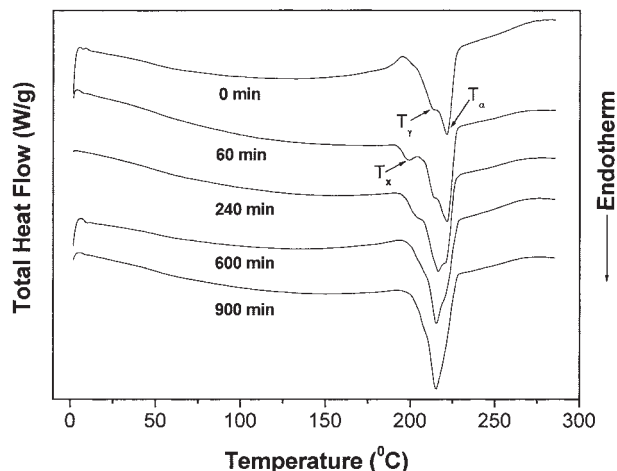


**Figure 7** MDSC traces of neat nylon 6 annealed at 190°C for different time durations.

annealed at 190°C for different times, the  $\gamma$ -form crystal of NCN5 specimen becomes the absolutely dominant crystalline phase, whereas the melting peak corresponding to  $\alpha$ -form crystal is much reduced and observed only as a shoulder at last. It has been reported that annealing can relieve some of the residual stress accumulated during process,<sup>33</sup> and consequently, the dominant  $\alpha$ -form crystals in NCN5 are able to rearrange to an increasingly favored  $\gamma$ -phase conformation because of the thermal activation provided by annealing and this phase conversion will become more prominent when enough annealing time is given. It has been reported by Berglund and co-workers<sup>34</sup> that the relatively high cooling rate also preferred forming less stable  $\gamma$  phase. (2) The peak temperature of  $\gamma$ -crystal,  $T_{\gamma}$ , remain fairly stationary and appear unaffected by the annealing time. But the annealing peak,  $T_x$ , was found to shift to higher temperature with increasing annealing time and finally overlapped with  $T_{\gamma}$ . Similar results for  $T_{\alpha}$ ,  $T_{\gamma}$  and  $T_x$  were also observed in the neat nylon 6 (Fig. 7). The dominant fractions of the  $\gamma$ -crystal in both NCN5 and nylon 6 samples annealed at 190°C as compared with those annealed at 170°C suggest that  $\gamma$ -crystal forms more readily during a higher temperature solid-state annealing.

The MDSC thermograms of NCN5, annealed at 240°C (melt-state annealing) for various durations, are shown in Figure 8. It can be seen from Figure 8 that only one endothermic peak was observed in NCN5, which corresponds to the  $\alpha$ -form crystal and no  $\gamma$ -phase was detected. This phenomenon is illustrated more clearly in Figure 9, which compares the nonreversing thermal events between NCN5 and nylon 6 during annealing at 240°C for 600 min. For NCN5 specimens, only two nonreversible events were detected. There is a strong exotherm centered at 215°C,

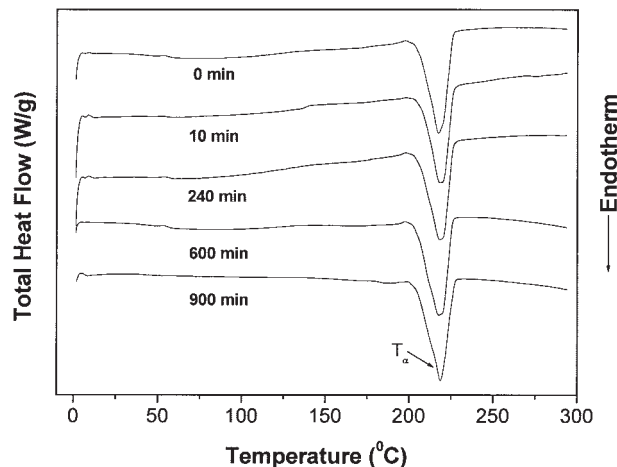


**Figure 8** MDSC traces of NCN5 annealed at 240°C for different time durations.

immediately followed by a sharp endothermic peak at 223°C, indicating that the  $\alpha$ -phase crystals undergo a process of crystal perfection during the heating scan and subsequently these higher melting species melt at 223°C.

For neat nylon 6 annealed at 240°C (Fig. 10), however, very different MDSC thermograms were obtained, where the  $\gamma$ -crystals were detected in all neat nylon 6 samples and  $\Delta H_{\gamma}$  of the endothermic shoulder peak was found to increase with increasing annealing time and the  $\Delta H_{\alpha}$  showed a decrease after annealing. The relative ratios between  $\Delta H_{\alpha}$  and  $\Delta H_{\gamma}$  in neat nylon 6 are illustrated clearly in Figure 11, which compares the changes in  $\Delta H_{\alpha}/\Delta H_{\gamma}$  as a function of annealing time. There is a rapid initial drop of the  $\Delta H_{\alpha}/\Delta H_{\gamma}$  value followed by a gradual decrease after about 240 min. This means the annealing at 240°C induces the formation of the  $\gamma$ -phase of nylon 6 samples. More-

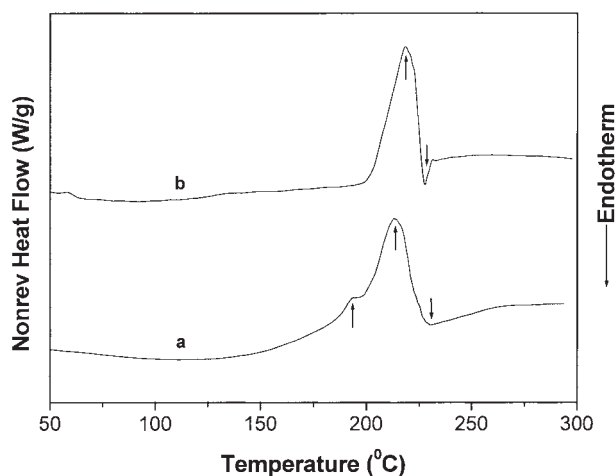


**Figure 9** Nonreversing MDSC data of (a) nylon 6 and (b) NCN5 annealed at 240°C for 600 min.

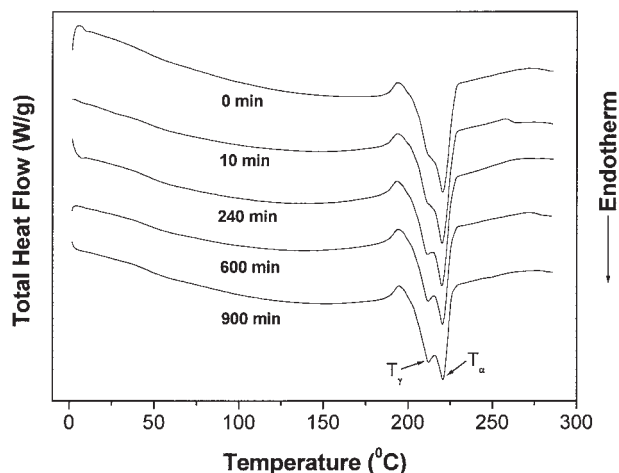


Figure 10 MDSC traces of neat nylon 6 annealed at 240°C for different time durations.

over, the differences between neat NCN5 and nylon 6 can be seen more clearly from the nonreversing MDSC signal of both samples in Figure 9. Two crystalline perfection processes have been observed for neat nylon 6 in the nonreversing exothermic signal that corresponds to the crystal perfection process of both  $\alpha$ -crystal and  $\gamma$ -crystal.

To further confirm the MDSC results obtained, XRD analysis was carried out using the annealed samples that were prepared using the same procedures as for MDSC measurements. Figure 12 illustrates WAXD scans of nylon 6/clay nanocomposites annealed for 600 min at 170, 190, and 240°C, respectively. The XRD results agree well with the MDSC observations.

## CONCLUSIONS

The differences in polymorphism and thermal behavior between NCN5 and nylon 6 have been compar-

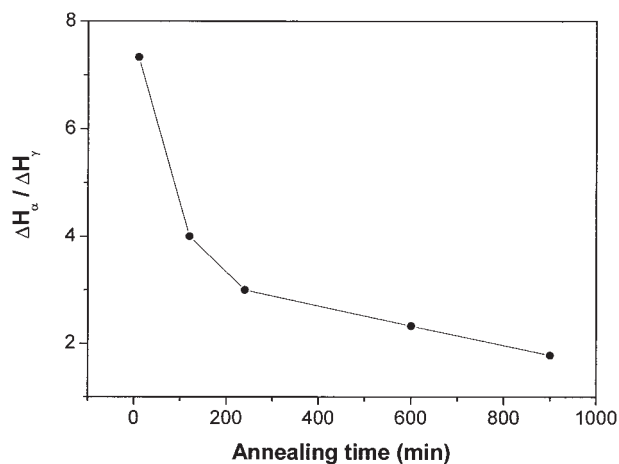


Figure 11 Changes in the content of  $\gamma$ -phase and  $\alpha$ -phase as a function of annealing time (annealed at 240°C).

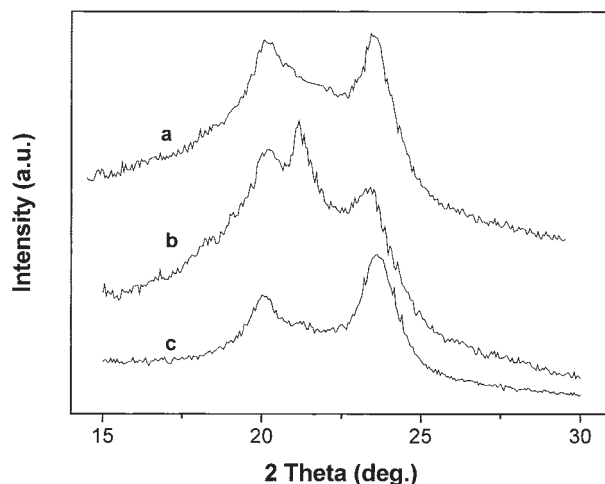


Figure 12 WAXD patterns of NCN5 samples annealed at (a) 170°C, (b) 190°C, and (c) 240°C for 600 min.

tively studied and the effect of thermal history on the time evolution of the polymorphic structure of NCN5 and nylon 6 was also investigated. The polymorphic behavior and thermal property of both NCN5 and nylon 6 were found to depend on the thermal history of the specimen. Annealing in the solid state at 170°C is more favorable for the formation of the thermodynamically stable  $\alpha$ -crystal, whereas annealing in the solid state at 190°C could cause the phase conversion from the  $\alpha$ -phase to the  $\gamma$ -phase subjected to the annealing time. On the other hand, annealing in the melt state at 240°C has no significant effects on the structure of nanocomposite NCN5. For nylon 6 annealing in the melt state, however, the formation of  $\gamma$  crystal has been greatly enhanced with increasing the annealing time. The difference in polymorphism between neat nylon 6 and NCN5 reflected the complexity of the melting behavior of NCN5 system. Furthermore, a small endothermic peak appeared at low-temperature region was found to strongly depend on the thermal history.

## References

- Okada, A.; Kawasumi, M.; Kurauchi, T.; Kamigaito, O. *Polym Prepr* 1987, 28, 447.
- Usuki, A.; Kojima, Y.; Kawasumi, M.; Okada, A.; Fukushima, Y.; Kurauchi, T.; Kamigaito, O. *J Mater Res* 1993, 8, 1179.
- Burnside, S. D.; Giannelis, E. P. *Chem Mater* 1995, 7, 1597.
- Lee, D. C.; Jang, L. W. *J Appl Polym Sci* 1998, 68, 1997.
- Lincoln, D. M.; Vaia, R. A.; Wang, Z.; Hsiao, B. S.; Krishnamoorti, R. *Polymer* 2001, 42, 9975.
- Yano, K.; Usuki, A.; Okada, A.; Kurauchi, T.; Kamigaito, O. *J Polym Sci* 1993, A31, 2493.
- Yano, K.; Usuki, A.; Okada, A. *J Polym Sci* 1997, A35, 2289.
- Gilman, J. W. *Appl Clay Sci* 1999, 15, 31.
- Morgan, A. B.; Gilman, J.; Harris, W.; Jackson, C. L.; Wilkie, C. A.; Zhu, J. *Polym Mater Sci Eng* 2000, 83, 53.
- Komarneni, S. *J Mater Chem* 1992, 2, 1219.

11. Hill, P. G.; Foot, P. J. S.; Davis, R. *Synth Met* 1996, 76, 289.
12. Mark, J. E. *Polym Eng Sci* 1996, 36, 2905.
13. LeBaron, P. C.; Wang, Z.; Pinnavaia, T. J. *Appl Clay Sci* 1999, 5, 11.
14. Liu, L. M.; Qi, Z. N.; Zhu, X. G. *J Appl Polym Sci* 1999, 71, 1133.
15. Mathias, L. J.; Davis, R. D.; Jarrett, W. L. *Macromolecules* 1999, 32, 7958.
16. Wu, T. M.; Liao, C. S. *Macromol Chem Phys* 2000, 201, 2820.
17. Varlot, K.; Reynaud, E.; Kloppfer, M. H.; Vigier, G.; Varlet, J. *J Polym Sci Part B: Polym Phys* 2001, 39, 1360.
18. Wu, T. M.; Chen, E. C.; Liao, C. S. *Polym Eng Sci* 2002, 42, 1141.
19. LeBaron, P. C.; Wang, Z.; Pinnavaia, T. J. *Appl Clay Sci* 1999, 15, 11.
20. Vaia, R. A.; Price, G.; Ruth, P. N.; Nguyen, H. T.; Lichtenhan, J. J. *Appl Clay Sci* 1999, 15, 67.
21. Kojima, Y.; Matsuoka, T.; Takahashi, H.; Kurauchi, T. *J Mater Sci Lett* 1993, 12, 1714.
22. Liu, X.; Wu, Q. *Eur Polym Mater* 2002, 38, 1383.
23. Fornes, T. D.; Paul, D. R. *Polymer* 2003, 44, 3945.
24. Maiti, P.; Okamoto, M. *Macromol Mater Eng* 2003, 288, 440.
25. Okada, A.; Fukushima, Y.; Kawasumi, M.; Inagaki, S.; Usuki, A.; Sugiyami, S.; Kurauchi, T.; Kamigaito, O. U.S. Pat. 4,739,007 (1998).
26. Kata, M.; Usuki, A. In *Polymeric-Clay Nanocomposites*; Pinnavaia, T. J., Ed.; JWS: England, 2000.
27. Illers, H. K.; Haberkorn, H.; Simak, P. *Makromol Chem* 1972, 158, 285.
28. Cheng, L. P.; Lin, D. J.; Yang, K. C. *J Membr Sci* 2000, 172, 157.
29. Illers, H. K.; Haberkorn, H. *Makromol Chem* 1971, 142, 31.
30. Bonnet, M.; Rogausch, K. D.; Petermann, J. *Colloid Polym Sci* 1999, 277, 513.
31. Liu, T. X.; Yan, S. K.; Bonnet, M.; Rogausch, J. *J Mater Sci* 2000, 35, 5047.
32. Liu, T. X.; Petermann, J. *Polymer* 2001, 42, 6453.
33. Khannam, Y. P. *Macromolecules* 1992, 25, 3298.
34. Wu, Q.; Liu, X.; Berglund, L. A. *Macromol Rapid Commun* 2001, 22, 1438.